Area-selective formation of Si nanocrystals by assisted ion-beam irradiation during dual-ion-beam deposition

Jae Kwon Kim, Kyu Man Cha, Jung Hyun Kang, Yong Kim,[a] Jae-Yel Yi, Tae Hun Chung, and Hong Jun Bark
Department of Physics, Dong-A University, Hadan-2-dong, Sahagu, Pusan 604-714, Korea

(Received 10 February 2004; accepted 27 June 2004)

We investigate the effect of Ar-ion-beam irradiation during the deposition of SiO_x films by dual-ion-beam deposition system. Ion-beam irradiation effectively increases the oxygen content, x, in SiO_x films indicative of the preferential sputtering of Si phase as compared to SiO_2 phase in SiO_x films. We observe the intense photoluminescence from nonirradiated sample after postdeposition annealing at 1100 °C indicating the formation of Si nanocrystals as shown by a cross-sectional transmission electron microscope. However, the increased oxygen content in ion-beam-irradiated sample results in small optical volume of small Si nanocrystals not sufficient for yielding appreciable photoluminescence intensity after postdeposition annealing. The property is utilized for achieving the area-selective formation of Si nanocrytals by inserting a shadow mask in assist ion beam during deposition. © *2004 American Institute of Physics*. [DOI: 10.1063/1.1785864]

Since the first discovery of the light emission from porous silicon,[1] the interest toward Si-based optoelectronics has rapidly increased. Due to the better compatibility with standard ultralarge-scale integrated circuit (ULSI) processes, Si nanocrystals in a dielectric matrix have gained much interest. The standard approach for the formation of Si nanocrystals is the utilization of the prolonged annealing of SiO_x ($x<2$) films at temperatures higher than 900 °C. During annealing, phase separation and precipitation take place owing to the energetic stability of Si and SiO_2 phases. The various attempts for the growth of SiO_x films include ion implantation,[2] chemical vapor deposition,[3–6] reactive evaporation,[7] cosputtering,[8] ion-beam sputtering,[9] etc. SiO_x ($x\sim1$) films yield highly luminescent nanocrystals with large density regardless of growth methods. The previous methods are not area selective and thereby nanocrystals are precipitated in whole deposited area. However, the area-selective technique in forming Si nanocrystals may offer a processing advantage in future ULSI processes. In this letter, we report the area-selective formation technique of Si nanocrystals by using ion-beam irradiation during dual-ion-beam deposition (DIBD).

SiO_x films were deposited by employing a DIBD system. A DIBD system consists of two Kaufman-type broad-beam ion sources. Ultrapure Ar gas was used for source gas for ion-beam generation. Primary ion source of 2.5 cm diameter with the incident angle of 65° served as a sputtering ion source as illustrated in Fig. 1. P-type (100) silicon wafer (resistivity ~10 Ω cm) was used as a sputtering target. The beam energy and beam current of the primary ion source were 750 eV and 7 mA, respectively. An assisted-ion source of 6 cm diameter with the incident angle of 37° was used. The beam current of the assisted-ion source was 10 mA and beam energy was variable parameter (0–200 eV). 10% Ar-diluted O_2 gas was introduced into the deposition chamber for a reactive deposition. The operating pressure was kept at 6×10^{-4} Torr while the partial pressure of O_2 gas was variable parameter. No intentional heating was applied on substrate during deposition. SiO_x films were deposited for 2–4 h on 3 in. p-type (100) Si wafer (resistivity ~10 Ω cm) after standard cleaning sequence to remove organic and inorganic surface contaminants.

Deposited SiO_x films were subsequently annealed at 1100 °C for 2 h in an N_2 ambient. They were further annealed at 450 °C for 3 h in a forming gas (N_2 90%, H_2 10%) for H_2 passivation. Photoluminescence (PL) was excited by 488 nm Ar^+-ion laser (30 mW and ~1 mm beam diameter). PL was dispersed by a 0.5 m monochrometer (Dongwoo optron DM500). The PL signal was detected by a photomultiplier tube (Hamamatsu R928). The observed PL spectra were corrected using a tungsten–halogen lamp. All measurements were done at room temperature. The cross-sectional transmission electron microscope (TEM) image was observed by using a JEOL JEM-2010 equipment through a standard preparation technique. The bonding configurations in oxide matrix were measured by Fourier transform infrared spectroscopy [(FTIR) Biorad Excalibur FTS-3000]. According to Pai *et al.*,[10] Si—O—Si stretching vibration frequency shifts linearly with the oxygen content, x, provided that the film is homogeneous. Therefore, the position of the Si—O—Si stretching vibration frequency was used in determining the oxygen content, x, in SiO_x film.

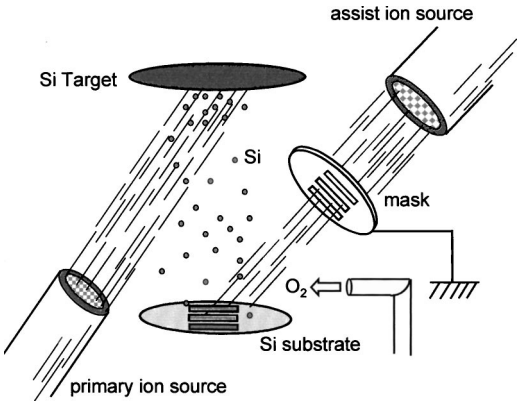

FIG. 1. Schematic illustration of dual-ion-beam deposition with a grounded shadow mask.

[a]Electronic mail: yongkim@daunet.donga.ac.kr

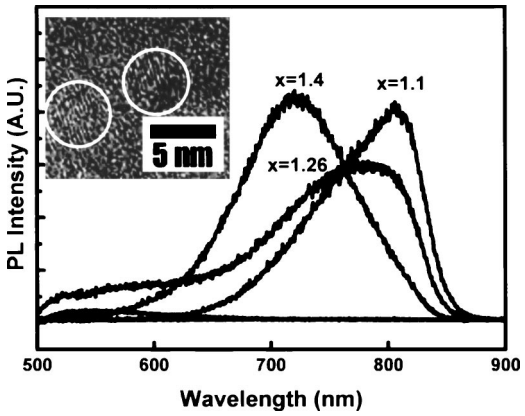

FIG. 2. PL spectra of SiO_x films with various oxygen content, x, after the high-temperature N_2 annealing and additional forming gas annealing. The inset shows the cross-sectional TEM image of $SiO_{1.26}$ film containing nanocrystals. White boundaries in the inset are a guide for the eyes.

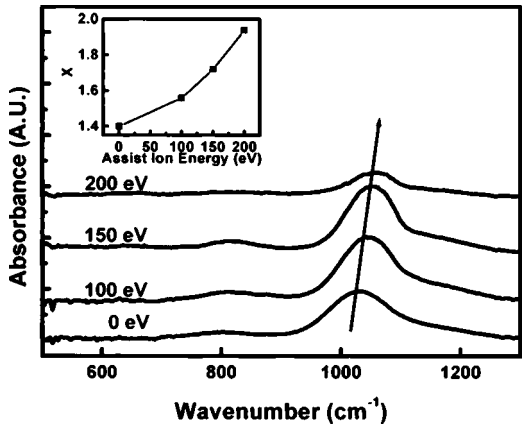

FIG. 3. Infrared spectra of SiO_x films irradiated with assisted ions of various ion-beam energies. O_2 partial pressure was 1.4×10^{-5} Torr during deposition. The spectra are shifted for clarity. The arrow indicates the variation of Si—O—Si stretching vibration with assisted-ion-beam energy. The inset shows the variation of x as a function of assisted-ion-beam energy.

First, we grew several SiO_x films ($0.56\leqslant x\leqslant 1.6$) with various oxygen contents by adjusting the O_2 partial pressure from 0.6×10^{-5} Torr to 1.6×10^{-5} Torr. In this case, assisted-ion source was not activated. The oxygen content was linearly proportional to the partial pressure of introduced oxygen. Therefore, the DIBD technique is quite reliable in preparing SiO_x films with a desired oxygen content. After postdeposition annealing, we observe PL emissions for samples in the compositional window of $1.1\leqslant x\leqslant 1.4$ as shown in Fig. 2. The size of Si crystallites critically depends on the oxygen content in the film and exceeds the size of nanocrystal for having an appreciable quantum confinement effect for the films with $x<1.1$. On the other hand, the small optical volume of nanocrystals for the films with $x>1.4$ is not sufficient for yielding reasonable PL intensity. As is observed in Fig. 2, PL shows a blueshift as x increases. This is due to the stronger quantum confinement effect as the size of Si nanocrystals decreases. The inset shows the cross-sectional TEM image of typical nanocrystals (~5 nm diameter) found in SiO_x layer with $x=1.26$, and supports the fact that observed PL is attributable to Si nanocrystals in the films.

The assisted-ion beam has been utilized to significantly enhance and control the properties of the film. The effect of assisted-ion-beam irradiation is the densification of film and the reduction of film stress. Assisted ions preferentially sputter deposits and contaminants usually with low bonding energy.[11] However, in this study, assisted ions are used for the modification of SiO_x properties.

Figure 3 shows the FTIR spectra for deposited SiO_x films with an O_2 partial pressure of 1.4×10^{-5} Torr by varying the beam energy of an assisted-ion source. The IR band found at around 1050–1080 is attributed to the Si—O—Si stretching vibration. The Si—O—Si stretching vibration frequency gradually shifts as the ion-beam energy increases. The inset of Fig. 3 shows x determined from Pai's relation[10] as a function of assisted-ion-beam energy. The inset also shows the superlinear increase of x with ion-beam energy, and the film grown under 200 eV ion-beam irradiation is almost close to the stoichiometric SiO_2 film. The microstructure of SiO_x films has been discussed either by the random mixture model (RMM)[12] or random bond model (RBM).[13] As discussed by Lombardo *et al.*[4] from the detailed x-ray photoelectron spectroscopy study, a combined model reflecting both models accounts for the true microstructure of SiO_x film. The tendency observed in Fig. 1 is explained in terms of the preferential sputtering of the Si phase due to the higher sputtering yield as compared to the SiO_2 phase when considering RMM as the microstructure of SiO_x film. The other possibility is due to the enhancement of the surface process which increases the rate of oxygen incorporation. However, we observe a significant reduction in film thickness with assisted-ion-beam irradiation. The model of the preferential sputtering would be more plausible. Argon sputtering can introduce both bulk and surface atomic displacements. However, the bulk atomic displacement should be removed with annealing at 1100 °C.[14]

Because of the narrow compositional window of $1.1\leqslant x\leqslant 1.4$ for having an appreciable PL, the films grown under ion irradiation will not show any appreciable PL. This is confirmed in Fig. 4. SiO_x films under ion-beam irradiation show only a weak PL band at around 550 nm presumably due to matrix defects similar to the report by Min *et al.*[15] The controllability of x in SiO_x films by assisted-ion-beam irradiation can be utilized for area-selective formation of Si nanocrystals. As illustrated in Fig. 1, a shadow mask is inserted in the assisted-ion beam. The mask is grounded to prevent a charging effect. Otherwise, assisted ions would not reach the sample surface due to Coulomb repulsion. A preliminary experiment employs a mask having three rectangular holes and an ion beam with 200 eV ion energy is directed

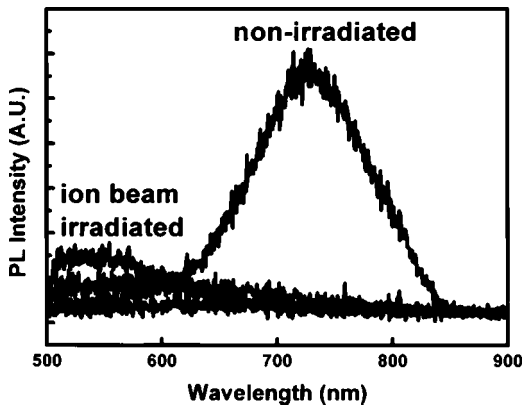

FIG. 4. PL spectra of SiO_x films with and without ion-beam irradiation.

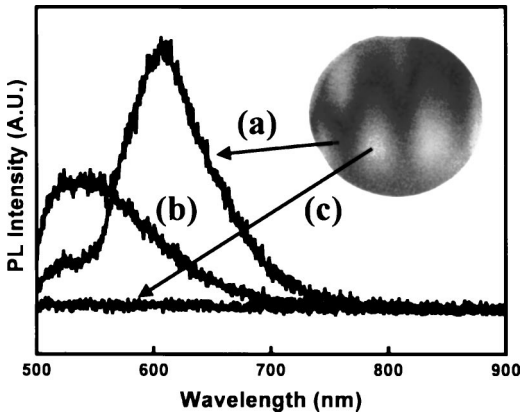

FIG. 5. PL spectra recorded from the different parts of 3 in. sample grown with a shadow mask. O_2 partial pressure was 1.4×10^{-5} Torr during deposition. The photograph shown in the inset is the photograph of 3 in. sample after the deposition. (a) and (c) are nonirradiated and irradiated regions, respectively. (b) is the transition region between (a) and (c).

to a 3 in. Si wafer through the holes during DIBD. Figure 5 shows the PL spectra recorded from the different parts of 3 inch SiO_x sample after the deposition of SiO_x with the same partial pressure in Fig. 4. The inset in Fig. 5 shows the photograph of a 3 in. SiO_x sample. Due to the refractive index alteration by ion-beam irradiation, the mask pattern is clearly discernable to the naked eye. However, the pattern is distorted and, specifically, the pattern of the nonirradiated region is narrowed due to the significant spread of assisted ions after escaping from the rectangular hole. The PL spectrum from the nonirradiated region shows the maximum intensity at 615 nm indicating the blueshift of 115 nm compared to PL from the nonirradiated sample shown in Fig. 4. The result indicates that the nominally nonirradiated region is actually affected by ion-beam irradiation resulting in the increase of x. The central part of irradiated region shows no PL as expected. The transition region between the nonirradiated and irradiated regions shows PL centered at 550 nm. To check the other possible reasons for PL variation, we have conducted a series of experiments including atomic force microscope measurements for surface roughness, and energy dispersive x-ray spectrum measurements for the contamination from mask material (SUS 304 UHV-accessible stainless steel). No significant differences between irradiated and nonirradiated regions have found.

To conclude, we have demonstrated the area-selective formation of Si nanocrytals by inserting a shadow mask in the beam from an assisted-ion source during DIBD. Ion-beam irradiation results in the increase of the oxygen content in SiO_x films due to the preferential sputtering of Si. By suitable control of the oxygen content, area-selective formation of Si nanocrystals is realized after postdeposition annealing. Though preliminary results show a spread of ion beam and distortion of the exposed pattern, the technique developed here may offer a process advantage during ULSI processed when optimized.

This work was supported by Grant No. R05-2002-000065-0 from the Basic Research Program of the Korea Science and Engineering Foundation.

[1] L. T. Canham, Appl. Phys. Lett. **57**, 1046 (1990).
[2] K. S. Min, Ph.D thesis, Caltech, CA, 2000.
[3] F. Iacona, G. Franzo, and C. Spinella, J. Appl. Phys. **87**, 1295 (2000).
[4] S. Lombardo and S. U. Campisano, Mater. Sci. Eng., R. **17**, 281 (1996).
[5] S. Lombardo, S. Coffa, C. Bongiorno, C. Spinella, E. Castagna, A. Sciuto, C. Gerardi, F. Ferrari, B. Fazio, and S. Privitera, Mater. Sci. Eng., B **69-70**, 295 (2000).
[6] H. J. Cheong, J. H. Kang, J. K. Kim, Y. Kim, J-Y. Yi, T. H. Chung, and H. J. Bark, Appl. Phys. Lett. **83**, 2922 (2003).
[7] M. Zacharias, J. Heitmann, R. Scholz, U. Kahler, M. Schmidt, and J. Blasing, Appl. Phys. Lett. **80**, 661 (2002).
[8] M. Fujii, S. Hayashi, and K. Yamamoto, Jpn. J. Appl. Phys., Part 1 **30**, 687 (1991).
[9] J.-S. Bae, S.-H. Choi, K. J. Kim, and D. W. Moon, J. Korean Phys. Soc. **43**, 557 (2003).
[10] P. G. Pai, S. S. Chao, Y. Takagi, and G. Lucovsk, J. Vac. Sci. Technol. A **4**, 689 (1986).
[11] J. J. Cuomo, S. M. Rossnagel, and H. R. Kaufman, *Handbook of Ion Beam Processing Technolog* (Noyes, Park Ridge, NJ, 1989).
[12] H. R. Philipp, J. Non-Cryst. Solids **8**, 627 (1972).
[13] R. J. Temkin, J. Non-Cryst. Solids **17**, 215 (1975).
[14] C.-J. Tsai, T. Vreeland, Jr., and H. Atwater, Appl. Phys. Lett. **64**, 434 (1994).
[15] K. S. Min, K. V. Shcheglov, C. M. Yang, H. Atwater, M. L. Brongersma, and A. Polman, Appl. Phys. Lett. **69**, 2033 (1996).